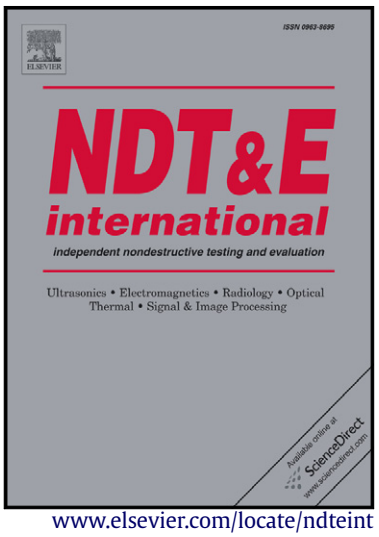

MATERIAL ENABLED THERMOGRAPHY

F. Pinto, F.Y. Maroun, M. Meo

PII: S0963-8695(14)00077-2
DOI: http://dx.doi.org/10.1016/j.ndteint.2014.06.004
Reference: JNDT1618

www.elsevier.com/locate/ndteint

To appear in: *NDT&E International*

Received date: 22 October 2013
Revised date: 9 June 2014
Accepted date: 11 June 2014

Cite this article as: F. Pinto, F.Y. Maroun, M. Meo, MATERIAL ENABLED THERMOGRAPHY, *NDT&E International*, http://dx.doi.org/10.1016/j.ndteint.2014.06.004

MATERIAL ENABLED THERMOGRAPHY

*F.Pinto, F.Y. Maroun, M. Meo**

Department of Mechanical Engineering, University of Bath, UK

*corresponding author: m.meo@bath.ac.uk

Abstract

This paper is focused on the analysis of a novel structural health monitoring technique based on the inclusion of a thermoresistive network within the structure of a traditional CFRP laminate. By exploiting the thermoelectrical properties of shape memory alloys (SMA) it is possible to employ them as an embedded heat source to rapidly identify the presence of internal defects in composite structures by monitoring the time history of the superficial thermal contrast. The sensitivity of the methodology was evaluated by testing several samples characterised by embedded defects in different positions and with different sizes, together with an analysis of the effect of the position of the SMA grid and the intensity of the feeding current. The results obtained were compared with traditional NDT inspections such as ultrasonic C-Scan and Shearography and showed that material-enabled thermography is able to give results comparable with other techniques, saving inspection time and reducing the total costs of the analysis. In addition, because the only requirements for the test are the presence of an embedded heat source and simple electrical contacts, the inspection does not need any external heaters, therefore it is possible to rapidly monitor the health status of complex parts without dismounting them from the structure.

Introduction

The rapid development of composite materials during the last two decades has underlined the necessity for new materials characterised by improved mechanical properties in order to extend their fields of applications. However, one of the most severe disadvantages of composite structures is constituted by the weak interfacial strength between the laminae under compressive loads which makes them sensible to impact damage, thus leading to the generation of barely visible impact damage (BVID), microcracks and delaminations.

Over the past years, a considerable amount of research has been devoted to evaluate an effective solution to this issue, aimed towards the improvement of the impact resistance of composite structures [1-3]. According to the literature, this can be achieved following different approaches, depending on the typology of intervention on the material structure. A first approach consists is the modification of one of the components of the material in order to increase its specific properties, reducing its weaknesses, thus improving the compatibility between the different phases that form the composite structure. Strengthen mechanisms such as matrix toughening [4], interface toughening [5] and fibres surface modification [6] belong to this category as they operate by increasing the properties of one or more existing phases within the material structure.

On the other hand, a different approach involves the hybridisation of the composite laminate through the embodiment of an additional engineered component characterised by specific functions, in order to exploit them to improve the impact resistance without affecting the other (desirable and needed) mechanical properties.

Hybrid materials reinforced with several engineered phases (such as hollow fibres [7], single and multi-walled carbon nanotubes [8, 9], graphene nanolayers and through-the-thickness reinforcements [2]) have been studied extensively during the last decade in order to evaluate how they can enhance the impact resistance of traditional laminates, showing good results in terms of energy absorption rate and structural vibrations damping .

Based on these considerations and following a similar methodology, impact properties can also be improved by embedding shape memory alloys (SMA) wires within a traditional laminate in order exploit their unique properties (superelasticity [10] and shape memory effect [11]), to reduce the extent of the internal delamination caused by low velocity impacts. These particular properties rise from the transitions between two different crystalline structures (martensite and austenite) that can be activated by applying temperature gradients or loading the material with an external force.

Several studies have been focused on the analysis of the enhanced mechanical properties of SMA based composites, and a comprehensive review has been carried out by Angioni et al [12]. However to this date, only few works have been focused on the possibility to exploit the presence of the internal network of SMA to enable additional non-structural functions for structural health monitoring (SHM).

Hideki et al [13] demonstrated that SMA can be used to evaluate the amount of damage in a hybridised GFRP by measuring the variation of the electrical resistance of embedded NiTi wires. The correlation between strain and electrical resistance variation for strain sensing is also the main objective of the work made by Cui et al [14] who demonstrated that for the purpose of strain sensing the material must be in its martensitic form so that this relationship is linear and independent from temperature. Localisation of the damaged areas and extent of the internal strain

distribution was also evaluated by Oishi et al [15] who analysed the acoustic emission signals generated from the austenite/martensite transformation.

Among the existing damage detection methods, active infrared thermography (IRT) represents one of the most promising non-destructive techniques, being able to detect subsurface defects for a wide variety of structural materials, including metals and composite media [16]. Contrary to passive thermography (which is based on the analysis of materials that are naturally at higher temperature than ambient), in the active approach an external stimulation is used to induce relevant temperature gradients that are recorded using an infrared camera, providing information regarding the integrity of structural components.

Indeed, as the presence of defects reduces locally the heat diffusion rate, when the surface temperature is analysed, damaged locations appears as areas of higher temperature than the rest of the sample [17, 18]. As a consequence, the thermal contrast can be used to locate invisible defects embedded within the material and measure their extent. Thermography can detect cracks in Glass Fibre Reinforced Plastics (GFRP) composites and it has been also proved to give good results in detecting voids, inclusions, and impact damage in Carbon Fibre Reinforced Plastics (CFRP) laminates [19]. However, some cracks could pass as undetected in case they are aligned parallel to the direction of heat flow.

The efficiency of the technique is strongly dependent on the way the thermal solicitation is given to the sample, being able to affect its feasibility and resolution. Indeed, according to the thermal stimulation, it is possible to identify three different kinds of thermographic inspection: pulses of light/heat in pulse thermography (PT), continuous heating (long pulse) in step heating thermography (SHT), and a sinusoidal

heat wave in lock-in thermography (LT). Nonetheless, all the above mentioned techniques require the use external heat sources such as infrared radiators or high-power photographic flashes, which makes them unsuitable for in situ aerospace applications as they require each part to be dismounted from the structure in order to set-up the heaters and proceed with the inspection.

The aim of this work is the analysis of a novel technique based on the use of SMA hybrid composites for in-situ NDT/SHM analysis of aerospace structures. The method combines the multi-physical properties of SMA composites with the benefits of thermal analysis, being able to guarantee the autonomous inspection of complex parts without the needs for expensive external heating devices. Indeed, the heat wave generated by a current passing through the internal SMA network will be delayed due to the presence of an internal damage, causing a difference in the apparent temperature on the sample's surface that is detected and captured using a thermal IR-camera (see Figure 1).

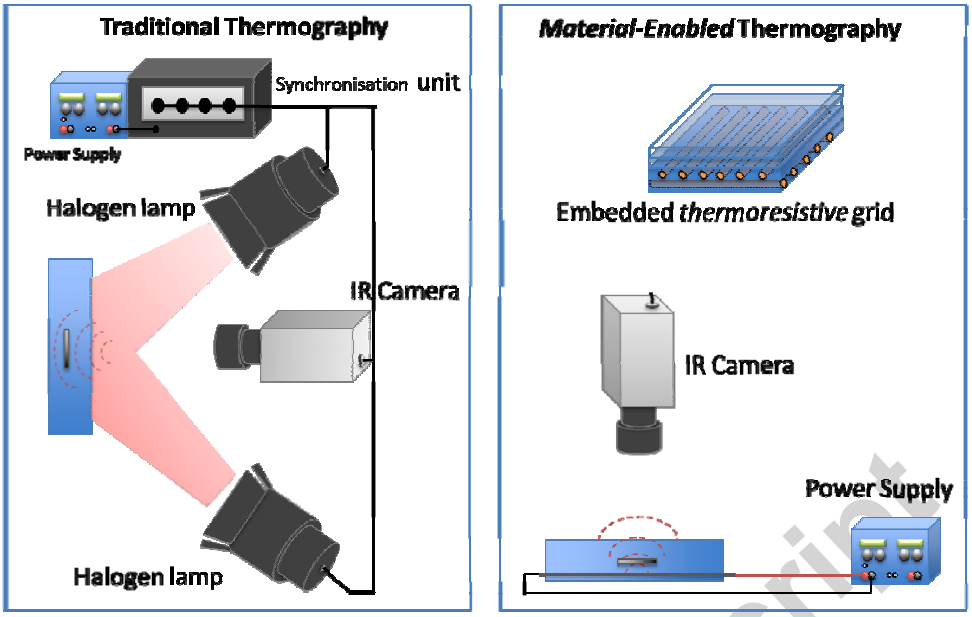

Figure 1 - Schematics of traditional active thermography (left side) and material enabled thermography (right side)

Samples characterised by different geometries were manufactured and investigated via in-situ thermography and the feasibility of the technique was analysed by detecting the presence of delaminations embedded at different depths and with different extents. A comparison with traditional NDT techniques such as C-Scan and shearography was carried out in order to analyse the advantages and disadvantages of the material enabled thermography.

Samples manufacturing and experimental set-up

Different samples were manufactured in order to validate the material-enabled thermography as an appropriate technique to be used as an in situ NDT/SHM system. The samples were manufactured using different configurations of SMA network, damage dimensions and specimens geometry.

Sample I was manufactured by laying-up 10 layers of T700 UD carbon fibres prepreg (Airtech, UK) following a $[0°,90°]_n$ stacking sequence. A network of 6 SMA wires was embedded between the third and fourth prepreg layers, with an inter-wire distance of 10 mm. In order to simulate the presence of an internal delamination, three squared Polytetrafluoroethylene (PTFE) patches characterised by different dimensions were included into the lamination sequence between the seventh and the eighth layers. As the presence of these patches locally hinders the reticulation of the polymeric chains during the curing reaction, the inclusion of Teflon inserts is a well-known technique to introduce artificial delaminations in a laminate structure, as reported in literature [20-22].

The dimensions of the patches used for Sample I are as follows: PTFE 1 (20 x 20 mm), PTFE 2 (10 x 10 mm) and PTFE 3 (5 x 5 mm). Figure 2 shows a schematic layout of the sample.

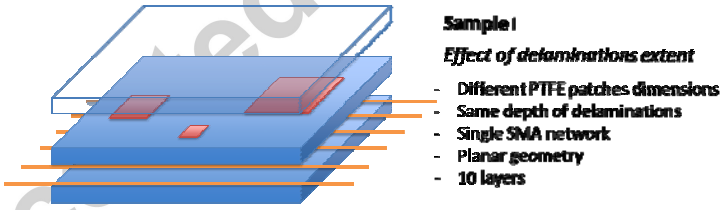

Figure 2 - Schematics of Sample I

The dependence of the position of the SMA network on the technique resolution was investigated by analysing the superficial response of the same PTFE patch recorded using two different SMA wires embedded at different depths within the laminate's thickness (Sample II) as heating source (Figure 3).

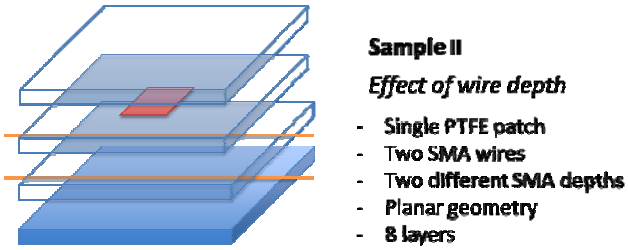

Figure 3 - Schematics of Sample II

Moreover, in order to analyse the effect on the thermal response of defects located at different positions along the z-axis, a third samples (labelled Sample III) was manufactured including two different PTFE patches in a 20 layers laminate. In particular, PTFE 1 was placed closer to the SMA network (between the 8th and 9th layers) while PTFE 2 was positioned closer to the top surface of the sample (between the 17th and 18th layers). Details of Sample III are presented in Figure 4.

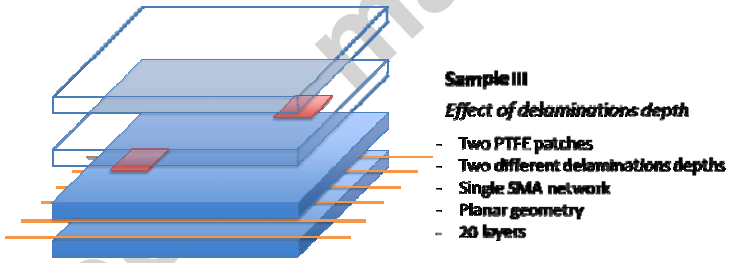

Figure 4 - Schematics of Sample III

Because of the presence of an embedded heat source within the laminate's structure, one of the biggest advantages of SMA enabled thermography over the traditional techniques is that structures characterised by complex geometries can be easily scanned without dismounting them to expose their surfaces to the heaters. This was validated by manufacturing Sample IV in the shape of a wing leading edge section ($[0,90]_{10}$)and using two squared PTFE patches (10 x 10 mm) embedded between the 17th and 18th layers as artificial defects (see Figure 5).

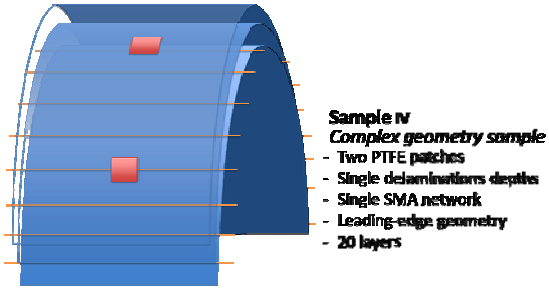

Figure 5 - Schematics of Sample IV

Figure 6 illustrates the experimental setup used to test the SMA enabled thermography. An electric current is passed through the wires for a period *t* of 3 seconds, heating up the samples via Joule effect. In order to guarantee an even distribution of the currents through the SMA network and a continuous thermal stimulation across the entire specimen, the wires were connected with a series of potentiometers on a circuit board fed through a power supply unit. Each SMA wire is plugged into a connector where a variable resistor regulates the amount of passing current. A series of switches determine the number of active SMA wires, depending on the resolution required from the test.

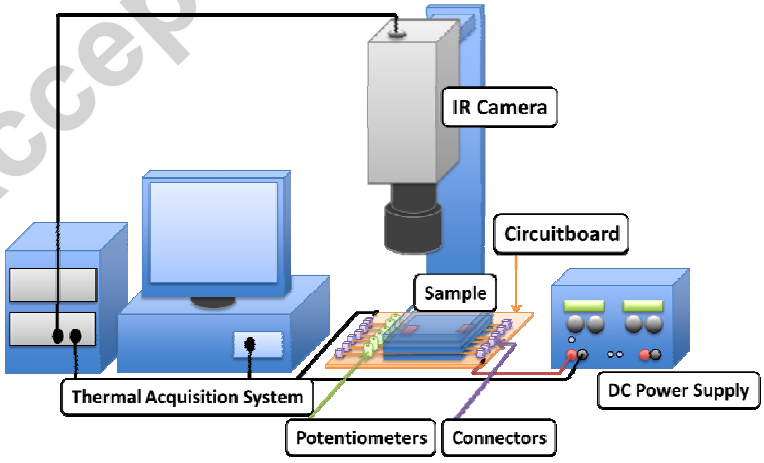

Figure 6 - Experimental Setup

Thermal images were captured using an electrically cooled IR camera (CEDIP) with a resolution of 320 x 240 pixel (width x height), maximum frame rate up to 150 Hz and a temperature sensitivity of 30 mK. All tests were conducted at ambient settings (25 °C). Step Heating Thermography (SHT) was the adopted technique used for the estimation of apparent temperature variation at the sample's surface.

Aside from the hidden flaws, there are other factors that could affect the acquired signal such as optical and electromagnetic noise, local variation of apparent temperature (heat noise) and uniformities due to imperfect heating. Therefore, in order to avoid any measuring errors, the first 100 frames of acquisition were subtracted and then the average for every pixel across the pre-activation frames was computed. This "background subtraction" allows focusing only on the thermal variation generated by the presence of internal defects, thus eliminating the effect given by others variables.

Results and discussions

The first series of tests was conducted on Sample I, in order to analyse the sensitivity of the technique when several defects (characterised by different dimensions) are embedded at the same depth within the laminate. As it is possible to see from Figure 7, each wire of Sample I (labelled from 1 to 6) was individually connected to a circuitboard in order to regulate the resolution of the thermograms acquired with the IR Camera. Indeed, feeding the circuitboard with a constant power, it is possible to divert a larger amount of current through a specific portion of the sample by switching off some of the SMA connectors, resulting in a local increase of the heat generated by Joule effect in that specific area. As a consequence, the resolution of the acquired

images is enhanced and smaller defects can be detected without the need to increase the total feeding current, thus keeping the total consumption of the system to low levels.

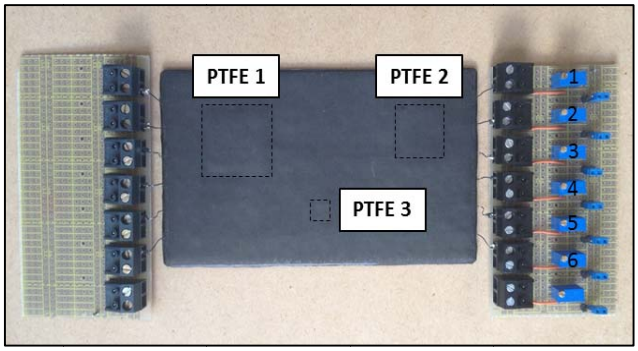

Total Current *[A]*	Number of wires	Current through each wire *[A]*
1.8	**6**	**0.3**
1.8	**5**	**0.36**
1.8	**3**	**0.6**
1.8	**2**	**0.9**

Figure 7 – Connection of Sample I to the circuitboard and summary of the experiments details

Figure 8 shows the thermal images obtained at the end of the Step Heating excitation (t = 3 s) for Sample I. As it is possible to see, the presence of the internal damage can be easily spotted from the large variation of the superficial thermal contrast. Indeed, because the internal delamination is characterised by lower values of thermal conductivity, the diffusion of the heat wave propagating through the sample's thickness is hindered by the Teflon patch, resulting in a variation of the apparent temperature in the surface portion that corresponds to the damaged area. Damage localisation is possible due to the low thermal diffusivity of the epoxy resin, which prevents the heat flow to spread immediately all over the specimen (as for metals) keeping it initially confined only in the area surrounding the NiTi wires. This ensures a relatively large time windows which is fundamental to evaluate the thermal gradients differences between damaged and undamaged areas.

Another important advantage of using the internal SMA network as a heating source is that by knowing the inter-wire distance it is possible to have a rough estimation of the extent of the internal damage.

Figure 8a illustrated the thermogram acquired feeding each wire with 0.3 A and it can be interpreted as a preliminary test where the entire SMA grid is connected to the power supply to perform a rapid scan of the specimen and identify relatively large delaminations. As it is possible to see from the image, the resolution of this "quick analysis" is good enough to identify the large defects 1 and 2, however, although some variations can be noticed in the area corresponding to PTFE3, the data recorded from the smallest damage can be easily misinterpreted. Therefore, the resolution of the scan was enhanced by limiting the number of the active wires to the ones surrounding the suspicious area and increasing the feeding current.

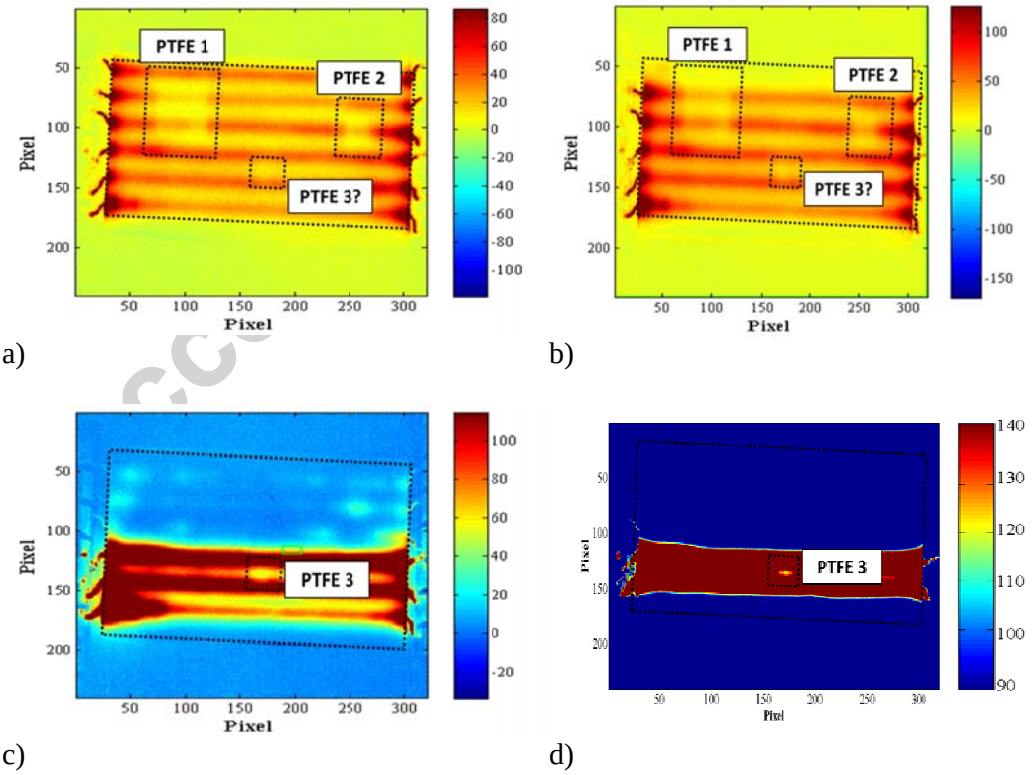

Figure 8 – Thermograms acquired from Sample I: a) quick-scan using 6 wires with 0.3 A each; b) 5 wires with 0.36 A each; c) 3 wires with 0.6 A each; d) 2 wires with 0.9 A each

Figure 8b shows the thermal image acquired for Sample I feeding 5 wires with 0.36 A each. Analysing the thermogram, it is possible to notice that because of the higher temperature gradient generated by the circulating current, the small damage (PTFE 3) starts to become visible. The resolution can be further increased by a further reduction of the number of wires used for the inspection, as showed in Figure 8c (3 wires with 0.6A for each wire) and Figure 8d (2 wires with 0.9 A for each wire)..

Data recorded from the IR camera are represented in Figure 9, where the response obtained from a damaged area (black continuous curve) is compared with the signal from an undamaged one (blue dashed curve).

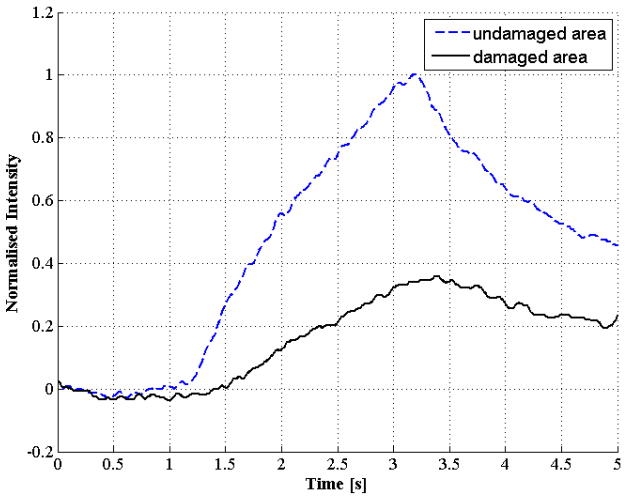

Figure 9 - Differences in the behaviour of the superficial thermal contrast between damaged and undamaged areas

As it is possible to see from the image, the presence of an internal damage strongly affects the thermal contrast by lowering the total amplitude of the recorded signal during the entire length of the test. Moreover, due to the variation of the thermal diffusivity in the damaged area, both heating and cooling ramps show strong phase differences and can be used to evaluate the presence of damage [23].

Effect of feeding current

The results obtained with Sample I underlined the importance of the feeding current on the feasibility and sensitivity of material-enabled thermography. Figure 10 represents the thermal response recorded from the same damaged area when an increasing amount of current is fed through the same NiTi wire. Analysing the results it is possible to observe that the hindering effect of the Teflon patch on the propagation of the heat wave is lowered when higher currents are used, showing an increase in the amplitude of the recorded signals (Figure 10a).

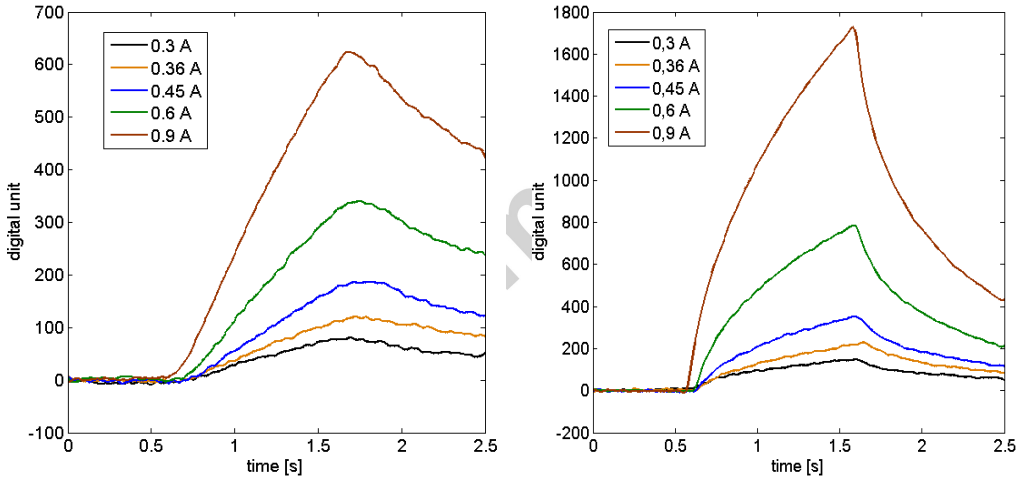

a) b)

Figure 10 – Effect of feeding current intensity on the response from a damaged area: a) apparent temperature variation behaviour with an increasing feeding current; b) contrast signals evaluated from the same data

However, in order to identify the exact location of the delamination on the xy plane, the readings from damaged areas ($W_{und_i}(t)$) must be compared with those acquired from undamaged areas placed along the same NiTi wire ($W_{dam_i}(t)$). This operation can be carried out using a contrast analysis ($C_{W_i}(t)$) according to the equation:

$$C_{W_i}(t) = \left| W_{und_i}(t) - W_{dam_i}(t) \right|$$

Contrast signals are represented in Figure 10b and the results are quite revealing. Indeed, although the absolute value of the signals acquired on damaged areas

increases, this effect is even higher for intact areas, therefore the contrast curves are shifted to higher values. Because the contrast curve represents the difference in the apparent temperature due to the presence of a damaged area, this gain enhances the scan resolution leading to the identification of smaller defects and delaminations.

Effect of the wire position

Apart from the feeding current, another important factor that plays a fundamental role in the general sensitivity of the technique, is the relative distance between the internal SMA grid, the internal delamination and the top surface. Indeed, the position along the z axis of the heating source (*d*) will determine the active area accessible to inspection as the defects positioned below the heat source cannot be detected from the external surface (although they could be detectable by acquiring the signals from the opposite surface). On the other side, when the heat source is embedded deeper in the material's thickness, the heat wave will need more time to propagate up to the top surface, reducing its intensity, thus lowering thermograms' resolution, as illustrated in Figure 11.

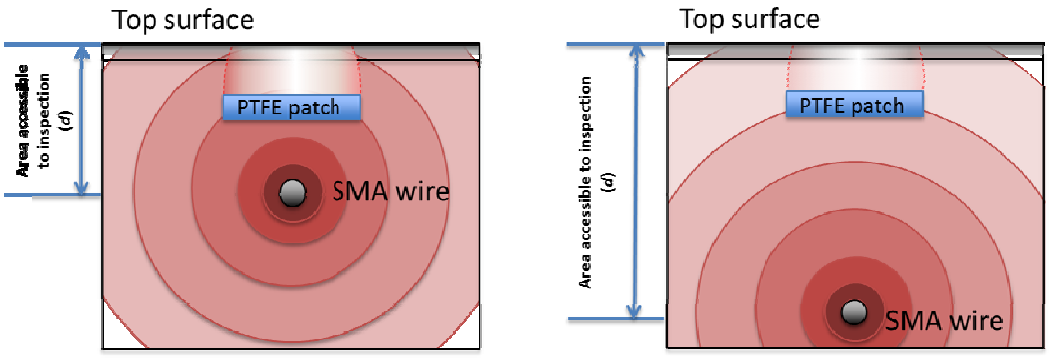

Figure 11 - Effect of the relative distance between the SMA grid, the damage position and the top surface

This hypothesis was experimentally confirmed from the tests conducted on Sample II, in which the thermal contrast generated from a single embedded damage, was

evaluated using two different SMA wires positioned at different depths (with $d_2<d_1$) as heating source and fed with the same current.

Analysing the thermograms it is possible to observe that the thermal response of the damaged area is only slightly affected by the reduction of d, while the data recorded from the undamaged areas are characterised by a higher increase of apparent temperature variation due to the increased proximity of the heat source with the external surface of the sample. This behaviour is clearly represented in the contrast analysis of Figure 12, from which it is possible to observe that the resolution of the system is almost doubled when the top SMA is used to heat the area surrounding the damage.

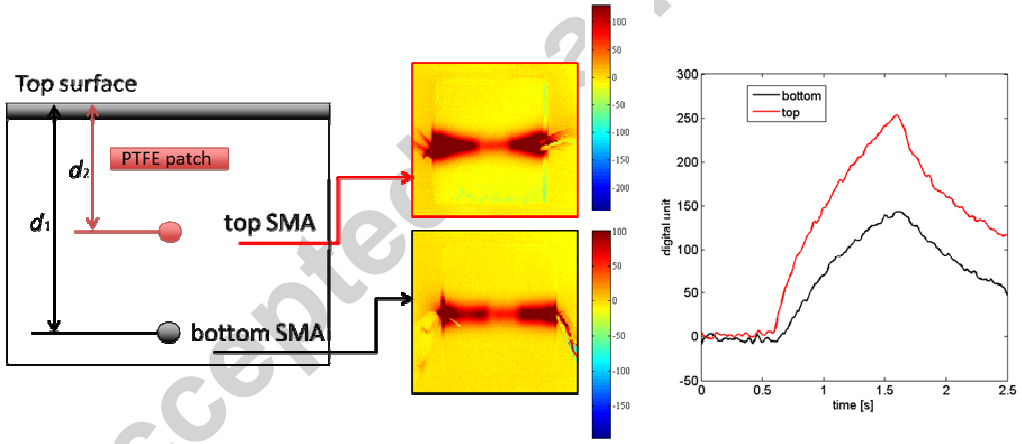

Figure 12 – Thermograms and contrast curves of the acquired signals recorded from Sample II using alternately Top and Bottom NiTi wire as embedded heat source

This dependence on the relative position of the SMA grid along the thickness on the resolution of the recorded thermograms represents another factor that can be exploited to tune the material-enabled thermal inspection. Indeed, as reported in several works [24-26], in order to optimise the energy absorption of hybrid composites under low-velocity impacts, multiple SMA layers must be embedded at different depths, usually

in the cross section and close to the top and bottom surfaces, as reported in [12]. The presence of this multi-layered structure can be exploited to further increase the feasibility of the inspection by tuning the feeding current according to the depth of the SMA network used as heat source to reduce the total power consumption of the system. For instance, defects embedded at deeper levels could be detected by using only the bottom SMA grid and feeding it with higher currents to balance the effect of the increased distance d in order to obtain a good thermal contrast between damaged and undamaged areas.

Effect of damage depth

Thermograms can be also useful to gain information regarding the relative z-positions of defects located at different depths in multi-damaged parts. Figure 13 shows the thermogram obtained from Sample III which is characterised by two PTFE patches separated by nine prepreg layers. Data recorded from the two damaged areas (points 1 and 2) are represented in Figure 13b, together with a comparison with the signal acquired from an undamaged area (point 3).

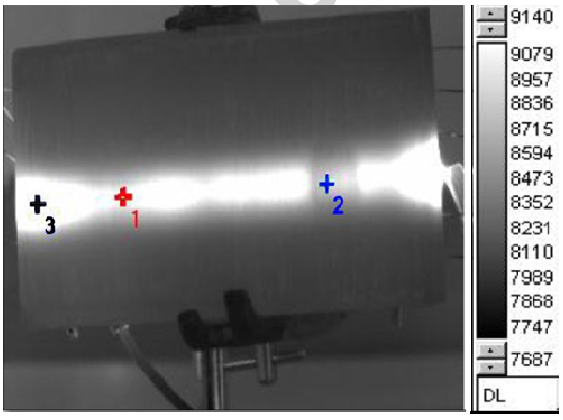

a)

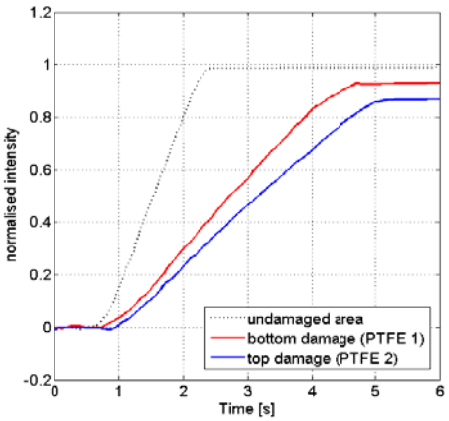

b)

Figure 13 - Thermogram and apparent temperature variation for Sample III

As it is possible to observe from the normalised curves, the intensity of the apparent temperature for the top damage (blue continuous line) is lower than the apparent temperature for the bottom one (red continuous line) by more than 10% due to the different location of the Teflon patches along the z direction. Indeed, as the heat wave propagates through PTFE 1, it has enough time to converge and overcome the delay caused by the presence of the Teflon patch before it hits the surface.

Analysing the curves it is possible to observe that the curve relative to the deeper damage is plotted closer to that of an undamaged area, therefore for a given feeding current there will be a maximum distance available for the scanning after which the signals acquired from damaged and undamaged area will be the same. However, as demonstrated previously, it is possible to enhance the difference between signals recorded from damaged and undamaged by increasing the amount of current used during the inspection thus enhancing the resolution on the system along the z-axis.

Effect of sample's geometry

The thermal image in Figure 14 represents the results of the tests conducted on Sample IV. As it is possible to see, despite the complex geometry, the damage embedded on the top curved portion of the sample was easily detected as in the case of the previous flat specimens. The graph in Figure 14b illustrates the time history of the apparent temperature difference between damaged (continuous black line) and undamaged (dashed magenta line) areas.

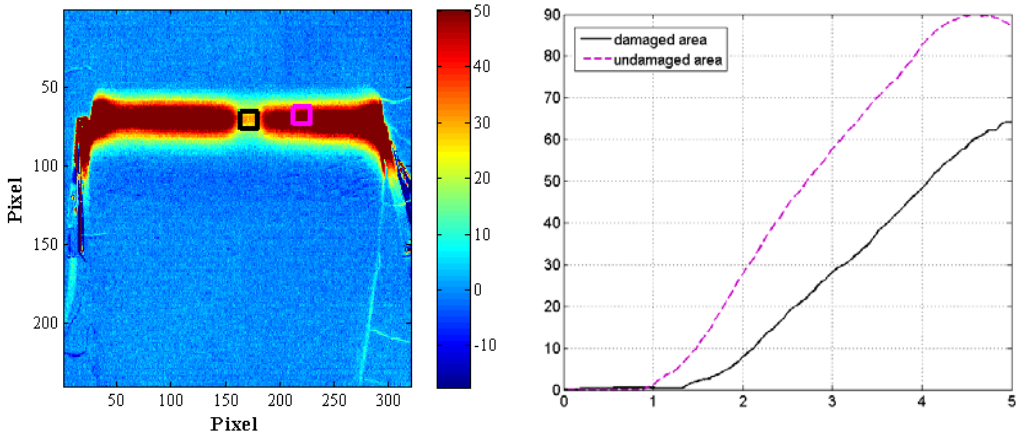

a) b)

Figure 14 - Thermogram and apparent temperature behaviour of damaged and undamaged portions of Sample IV

These results confirm how the material-enabled thermography can be used to inspect irregularly shaped structures without any geometrical limitations, showing good results in terms of resolution and sensitivity.

Comparison with C-Scan and Shearography

In order validate the feasibility of the material-enabled thermography, the data gathered from the previous tests were compared with traditional NDT techniques such as ultrasonic inspection and shearography.

C-Scan Analysis

The Ultrasonic NDT method used for sample inspection was the pulse-echo method. An Olympus 35 MHz pulse-receiver transducer (Panametrics) was employed to test the samples in an Ultrasonic Sciences Ltd (USL) C-Scan system. The inspection was carried out by submerging the specimen in a water tank and placing it on a glass plate

used as a reflective medium to distinguish the backwall echo from other echoed waves [27].

In order to compare the results obtained with the ultrasonic test in terms of both resolution and feasibility, two types of tests were performed. The first one was conducted in order to get a precise identification of the damaged areas, hence the time to complete the test was not a factor. The second test instead, was performed at a much faster rate in order to compare the results with the short time required to perform the material-enabled thermography inspection.

Figure 15a shows the C-Scan image of Sample I acquired in a time period of approximately 5 minutes. As it is possible from the results, all three PTFE patches can be easily identified and a rough evaluation of their extension can be performed analysing the contrast image. However, one of the big disadvantages of this technique is the time required for the scan which is significantly longer than the one required for material-enabled thermography (few seconds). In addition, the C-Scan machine could not inspect samples characterised by curved surfaces as the transducer can only move along the xy plane, limiting the inspection to planar samples.

Figure 15b shows the ultrasound acquisition obtained increasing the transducer speed to scan the entire sample in 1 minute. Analysing the results, it is possible to notice that when the scanning speed is increased, the resolution strongly decreases, lowering the feasibility of the inspection to unacceptable levels. Indeed, as it is possible to see from the image, some defects remain undetected (PTFE2) and others are detected with inaccuracy (PTFE1) resulting in a poor damage evaluation.

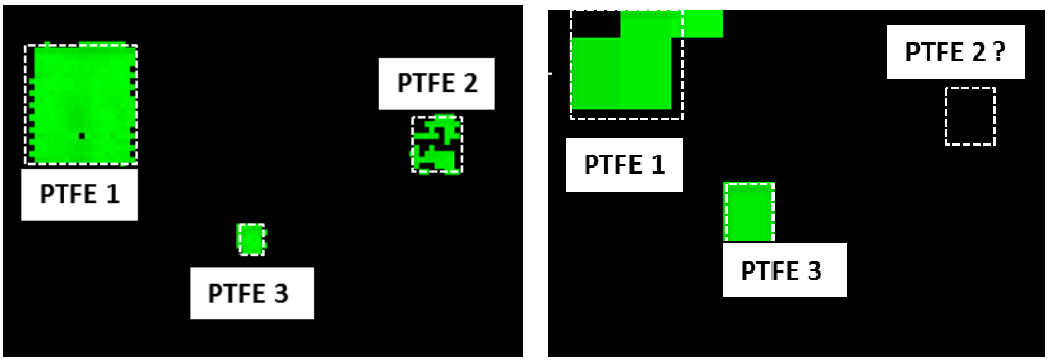

a) b)

Figure 15 - Ultrasound C-Scan image for Sample I : a) high resolution scan; b) high speed scan

Shearography

Shearography is an interferometric method that allows the measure of the derivatives of displacement on the surfaces of engineering components that has given good results for composite materials, as reported in many works present in literature [28-30]. The shearing device consists of a double-refractive crystal able to split one object point into two on the image plane when it is crossed by a beam of light, producing a couple of laterally sheared images (on the image sensor of the camera) whose interference creates a speckle pattern. The tested component is excited using a piezoelectric transducer and by comparing the speckle images acquired for both stressed and unstressed state, it is possible to obtain a low resolution image from which it is possible to calculate the gradient of the surface displacement, hence identify defects embedded within the laminate structure [31].

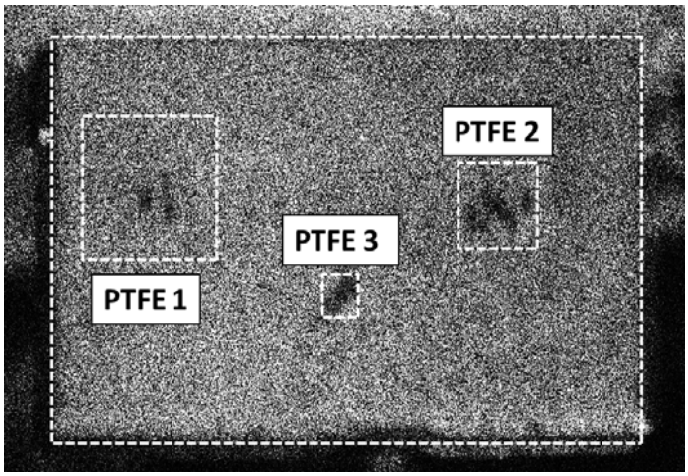

Figure 16 – Speckle pattern obtained with shearography on Sample I

Figure 16 represents the speckle pattern acquired for Sample I using a frequency of 69.5 kHz to excite the internal delaminations. As it is possible to observe from the image, shearography allows a good accuracy of the location for all three damaged areas (although it is not possible to evaluate their extents), however due to the presence of plate modes (which increase when higher excitations are employed) the results are difficult to analyse and could lead to misinterpretations and false positives [32]. Moreover, although this technique is generally quicker than C-Scan (the analysis is almost immediate), the time required for the frequency sweep can be relatively long as samples embedded at different depths will be excited at different frequencies.

Conclusions

This paper was aimed towards the investigation of the feasibility of a novel *material-enabled* methodology to assess the internal health status of complex composite structures based on the inclusion of thermo-resistive wires within a traditional laminate structure. In particular, the thermo-electrical properties of an embedded SMA network were exploited as an internal heat source for thermographic inspection to evaluate the presence of internal delaminations without the use of the large external

heaters or the complex signal processing techniques typical of traditional thermal analyses. In order to analyse the different factors that can influence the resolution and the sensitivity of the technique, several samples were manufactured, embedding defects with different dimensions and positioned at different depths along the z-axis. Results have demonstrated that internal delaminations can be spotted easily by analysing the thermograms acquired from an IR-Camera, giving good results in terms of position and spatial extent. Increasing the intensity of the current flowing through each wire it is possible to increase the resolution of the system. The sensitivity can be further tuned scanning selected portion of the structure by changing the number of wires used for the inspection and exploiting the insulating properties of the resin, thus lowering the total power requirements. Moreover, because the superficial thermal contrast is strongly affected by the time required for the propagation of the heat wave through the defect, the relative position between different damaged areas along the z-axis can be evaluated.

As several studies have proved that shape memory alloys are able to increase impact properties of composite structures, another important advantage of this technique is connected with the extreme flexibility of the manufacturing process which permits to embed the thermo-resistive grid also in parts characterised by complex shapes and geometries. A comparison with C-Scan and Shearography analyses have proved that the results obtained with this rapid novel technique can be compared with those obtained with traditional NDT techniques.

Acknowledgments

The authors would like to express their gratitude to Dr Simon Pickering for his support during this project and Dr Giovanni Orlando and Floriana Panzarella for their technical assistance.

References:

[1] Richardson M, Wisheart M. Review of low-velocity impact properties of composite materials. Composites Part A: Applied Science and Manufacturing. 1996;27(12):1123-31.
[2] Mouritz A, Leong K, Herszberg I. A review of the effect of stitching on the in-plane mechanical properties of fibre-reinforced polymer composites. Composites Part A: applied science and manufacturing. 1997;28(12):979-91.
[3] Cantwell W, Morton J. The impact resistance of composite materials—a review. composites. 1991;22(5):347-62.
[4] Morgan RJ, Jurek RJ, Yen A, Donnellan T. Toughening procedures, processing and performance of bismaleimide-carbon fibre composites. Polymer. 1993;34(4):835-42.
[5] Sain M, Suhara P, Law S, Bouilloux A. Interface modification and mechanical properties of natural fiber-polyolefin composite products. Journal of Reinforced Plastics and Composites. 2005;24(2):121-30.
[6] Gassan J, Bledzki A. Possibilities to Improve the Properties of Natural Fiber Reinforced Plastics by Fiber Modification–Jute Polypropylene Composites–. Applied Composite Materials. 2000;7(5-6):373-85.
[7] Hucker M, Bond I, Foreman A, Hudd J. Optimisation of hollow glass fibres and their composites. Advanced composites letters. 1999;8(4):181-9.
[8] Miyagawa H, Drzal LT. Thermo-physical and impact properties of epoxy nanocomposites reinforced by single-wall carbon nanotubes. Polymer. 2004;45(15):5163-70.
[9] Gou J, O'Braint S, Gu H, Song G. Damping augmentation of nanocomposites using carbon nanofiber paper. Journal of nanomaterials. 2006;2006.
[10] Meo M, Marulo F, Guida M, Russo S. Shape memory alloy hybrid composites for improved impact properties for aeronautical applications. Composite Structures. (0).
[11] Xu Y, Otsuka K, Nagai H, Yoshida H, Asai M, Kishi T. A SMA/CFRP hybrid composite with damage suppression effect at ambient temperature. Scripta materialia. 2003;49(6):587-93.
[12] Angioni SL, Meo M, Foreman A. Impact damage resistance and damage suppression properties of shape memory alloys in hybrid composites—a review. Smart Materials and Structures. 2011;20(1):013001.
[13] Nagai H, Oishi R. Shape memory alloys as strain sensors in composites. Smart materials and structures. 2006;15(2):493.
[14] Cui D, Song G, Li H. Modeling of the electrical resistance of shape memory alloy wires. Smart Materials and Structures. 2010;19(5):055019.
[15] Oishi R, Nagai H. Strain sensors of shape memory alloys using acoustic emissions. Sensors and Actuators A: Physical. 2005;122(1):39-44.

[16] Pickering S, Almond D. Matched excitation energy comparison of the pulse and lock-in thermography NDE techniques. NDT & E International. 2008;41(7):501-9.
[17] Maldague XP. Introduction to NDT by active infrared thermography. Materials Evaluation. 2002;60(9):1060-73.
[18] Carslaw HS, Jaeger JC. Conduction of heat in solids: Clarendon Press; 1959.
[19] McLaughlin P, McAssey E, Deitrich R. Non-destructive examination of fibre composite structures by thermal field techniques. NDT International. 1980;13(2):56-62.
[20] Avdelidis NP, Hawtin BC, Almond DP. Transient thermography in the assessment of defects of aircraft composites. NDT & E International. 2003;36(6):433-9.
[21] Ciampa F, Pickering S, Scarselli G, Meo M. Nonlinear damage detection in composite structures using bispectral analysis. p. 906402--8.
[22] Liu Y, Fard MY, Chattopadhyay A, Doyle D. Damage assessment of CFRP composites using a time–frequency approach. Journal of Intelligent Material Systems and Structures. 2012;23(4):397-413.
[23] Pinto F, Ciampa F, Meo M, Polimeno U. Multifunctional SMArt composite material for in situ NDT/SHM and de-icing. Smart Materials and Structures. 2012;21(10):105010.
[24] Kin-tak L, Hang-yin L, Li-min Z. Low velocity impact on shape memory alloy stitched composite plates. Smart Materials and Structures. 2004;13(2):364.
[25] Tsoi KA, Stalmans R, Schrooten J, Wevers M, Mai Y-W. Impact damage behaviour of shape memory alloy composites. Materials Science and Engineering: A. 2003;342(1–2):207-15.
[26] Khalili SMR, Shokuhfar A, Malekzadeh K, Ashenai Ghasemi F. Low-velocity impact response of active thin-walled hybrid composite structures embedded with SMA wires. Thin-Walled Structures. 2007;45(9):799-808.
[27] Hasiotis T, Badogiannis E, Tsouvalis NG. Application of Ultrasonic C-Scan Techniques for Tracing Defects in Laminated Composite Materials. Strojniški vestnik-Journal of Mechanical Engineering. 2011;57(3):192-203.
[28] Hung Y. Shearography for non-destructive evaluation of composite structures. Optics and lasers in engineering. 1996;24(2):161-82.
[29] Hung Y. Applications of digital shearography for testing of composite structures. Composites Part B: Engineering. 1999;30(7):765-73.
[30] De Angelis G, Meo M, Almond DP, Pickering SG, Angioni SL. A new technique to detect defect size and depth in composite structures using digital shearography and unconstrained optimization. NDT & E International. 2012;45(1):91-6.
[31] KRELL T, BRANDENBURG R, LAUTERBORN E. Comparative Investigation of Pulse Thermographic and Shearographic Testing of Composite Materials.
[32] Pickering S, Almond D. Comparison of the defect detection capabilities of flash thermography and vibration excitation shearography. Insight-Non-Destructive Testing and Condition Monitoring. 2010;52(2):78-81.

Highlights

- A material-enabled thermography system was developed
- Thermoresistive Shape memory alloy wires were embedded in CFRP laminate
- Accurate detection and sizing of defect was obtained